Romanian Reports in Physics **69**, 611 (2017)

CELLULAR DIFFERENTIATION EXACERBATES RADIATION SENSITIVITY *IN VITRO* IN A HUMAN DOPAMINERGIC NEURONAL MODEL

M. TEMELIE[1,2], C. MUSTACIOSU[1], M.L. FLONTA[2], D. SAVU[1*]

[1] "Horia Hulubei" National Institute of Physics and Nuclear Engineering, Department of Life and Environmental Physics, Magurele, Romania
[2] University of Bucharest, Department of Anatomy, Animal Physiology and Biophysics, Faculty of Biology, 91–95, Splaiul Independenţei, Bucharest, Romania
[*] *Corresponding author*: dsavu@nipne.ro

Received July 9, 2016

Abstract. UV radiations are well known cellular stressors. Following exposure to genotoxic factors the cells respond by molecular mechanisms aimed to repair the damages, block the proliferation or trigger cell death. Our study investigates how neuronal differentiation interferes with repair processes following UV-induced genotoxic stress, in a model of dopaminergic neurons (SH-SY5Y). Our work proved a higher level of DNA damage induced by UVC radiation in the dose range of 0.358–2.150 mJ/cm^2 in differentiated cells compared to the proliferative variants. Cellular viability decreases proportionally with the irradiation dose and post-exposure time and correlates with an increased apoptosis through caspase 3/7 activation. These effects were enhanced in differentiated cells in which we have seen increased DNA damage, incomplete repair, exacerbated viability loss and apoptosis induction.

Key words: UV, DNA damage, differentiation, neurons, SH-SY5Y.

1. INTRODUCTION

UV radiations induce various cellular lesions including oxidative stress, protein denaturation, and DNA damage [1]. In order to maintain the integrity and function of the genetic information, the cells develop mechanisms aimed to respond to these lesions. DNA Damage Response (DDR) is initiated by the sensor proteins leading to a complex transcription modulation involved in lesion repair, cell cycle control or cell death [1, 2]. With a diversity of DNA damages, multiple distinct repair mechanisms evolved. The most harmful cellular lesion – DNA double strand breaks (DSB) are alternatively managed by Homologus Recombination (HR) and Non-Homologus End-Joining (NHEJ), each of them with very complex mechanisms and specific features [2]. If the repair pathways are inefficient, the cells normally block the cell cycle, and eventually trigger apoptotic mechanisms, to avoid mutagenesis or carcinogenesis over generations [3].

Cellular differentiation involves specialization to certain functions concomitantly with a decreased proliferation [4]. Fully differentiated cells mainly synthesize the proteins required for their survival and their specific functions, the rest of the genome being inactive [5]. Various studies sustain a mutual relationship between DNA damage and cellular differentiation [6, 7]. On one side, the cellular differentiation interferes with DNA damage repair mechanisms, with divergent results accordingly to the cell type and study design [8–12], and on the other side, the cellular differentiation seems to be regulated as a response to DNA damage [13, 14].

Neuroblastoma SH-SY5Y represents an *in vitro* cell line, frequently used as a dopaminergic neuronal model, due to its characteristics [15, 16]. These cells are easily differentiated by removal of the serum supplement and addition of neuronal specific differentiation factors (*e.g.*: all-trans retinoic acid (RA), nerve growth factor (NGF), brain-derived neurotrophic factor (BDNF), insulin-like growth factor-1 (IGF-1)) [17–19]. Their differentiation is well characterized and can be observed by morphological changes, namely, the increased neurite length, number and complexity [17, 18], the presence of biochemical neuronal markers such as ß-III-tubulin, growth associated protein 43 (GAP43) [17], synaptic vesicle 2 protein (Sv2), NeuN, mature tau protein [18], acetylcholinesterase (ACHE), RET [19] or functional features including presence of synaptic and axonal vesicle transport [17, 20, 21] making them a good candidate for our study.

Here, we aim to address how cellular differentiation interferes with induction of DNA damage using a model of neuronal cells, the neuroblastoma cell line SH-SY5Y. We studied the DNA damage induction and the kinetic of subsequent processes either repair or apoptosis induction following UV irradiation, a well-known genotoxic agent.

2. MATERIALS AND METHODS

2.1. CELLULAR MODEL AND DIFFERENTIATION

The experiments were carried out on human neuroblastoma SH-SY5Y cells, received as a gift from by Dr. Nicoleta Moisoi, De Montfort University, Leicester, UK, used until passage 10, in DMEM/F12 (Biochrom, Germany), supplemented with 10% FBS (Biochrom, Germany), and 2 mM L-glutamine (Biochrom, Germany) in a humidified incubator at 37 °C, 5 % CO_2. Differentiation was induced by 7 days of growing in DMEM/F12 supplemented with 0.5 % FBS, 2 mM

L-glutamine and 10 μM all-trans retinoic acid (Sigma-Aldrich, Germany), changing the medium every 2–3 days.

The cells seeded for differentiation were plated at a low density in culture plates and let overnight to attach. Second day the medium was changed to differentiation medium, and incubated for 7 days renewing the medium at 2–3 days. At the end of the differentiation protocol, most of the cells presented robust expression of neuronal marker ß-III-tubulin as will be described later. The undifferentiated cells were plated the day before irradiation at a higher density, so that, in the moment of irradiation, all the cultures were at 70–80 % confluence. The irradiation was done simultaneously for proliferative cultures and the cells at the 7^{th} day of differentiation to reduce as much as possible variability in UV-exposure protocol.

Evaluation of cellular differentiation was done by morphological observation aimed to monitor progression of number, length, and complexity of the neurites and by immunofluorescence staining for a specific neuronal marker, beta-III-tubulin [22] and a control protein expressed in most cells, including neuronal precursors (actin). While proliferative cultures are known to express a low level of the neuronal marker, and a few simple neurite, during the differentiation, the expression sharply increases and the neurites multiply and elongate, forming a complex network [18].

The cultures were monitored daily using an inverted contrast microscope (CKX31, Olympus, Japan). At 3 and 7 days of culture, slides with cells were stained to assess the differentiation. The staining was done by the following protocol: 3 % paraformaldehyde (Sigma, Germany) 20 minutes, 0,25 % Triton X (Sigma, Germany) for 20 minutes, 5 % BSA (Jackson Immunoresearch, USA) for 1 hour, incubation with mouse IgG anti-beta-III-tubulin (Abcam, UK) 1:800 overnight at 4 °C, incubation with Alexa Fluor conjugated donkey anti-mouse IgG (Jackson Immunoresearch, USA) 1:200 and Texas Red conjugated Phalloidin (Invitrogen, USA) 1:100 for 1 hour, Hoechst 33342 2 μg/mL (Invitrogen, UK), 10 minutes. The slides were mounted with anti-fade mounting medium (ProLong Gold Antifade Reagent, Invitrogen, USA) and visualized using a fluorescence microscope (BX51, Olympus, Japan). Images were acquired using a Marlin F-046 CC camera.

2.2. UV IRRADIATION AND DOSIMETRY

The irradiation was performed using an UVItec Lamp, LF 206 at 245 nm, in standard culture medium. The dosimetry was established by a Solar Light co., PMA 2100 dosimeter using a quartz vessel filled with variable volumes of

medium, in order to establish the medium penetration of radiation applied, respectively the dose delivered to the cells. We have established a curve of medium height/dose delivered, for 1 minute exposure, with a height range of 0–7 mm of culture medium. Using Origin software, we have calculated the exponential decay equation needed for further calculation of dose applied to the cells in the culture vessels, resulting in: $Y(x) = 6.62\exp(-x/2.35) - 0.041$; $R^2 = 0.97741$ (Y = calculated dose; x = medium height).

Considering the volumes used later on in our experiments in the culture vessels and the surface area given by the manufacturer, we have calculated a height of 2.6 mm in the 96 well plates, using 100 μL of culture medium, and 3.1 mm in the 24 well plates, using 500 μL of medium so that the calculated doses that penetrate the medium and hit the cells were: 0.358 mJ/cm^2, 1.075 mJ/cm^2 and 2.150 mJ/cm^2 in the experiments performed in 24 well plates, correspond to 10 seconds, 30 seconds and 1 minute of exposure. In 96 well plates the doses we used were 0.850 mJ/cm^2 and 1.700 mJ/cm^2, applied in 30 seconds respectively, 1 minute of irradiation.

Immediately after the irradiation, the medium was renewed to remove the potential oxidative species formed from exposure of its components to UV.

2.3. VIABILITY ASSAY

Viability assay were performed using CellTiter 96 Aqueous One Solution Cell Proliferation Assay Kit (MTS) (Promega, USA), following the manufacturer instructions.

2.4. CASPASE 3/7 ASSAY

Caspase activation was evaluated by Caspase 3/7-Glo Assay (Promega, USA) following the manufacturer instructions. The signal recorded was normalized to the cell number given by viability recordings, similar to the method used by Stambolsky and his collaborators [23].

2.5. COMET ASSAY

Comet assay was performed under alkaline conditions according to the procedure of Singh *et al.* [24] with slight modifications.

Slides were analyzed using an image analysis system (Comet Assay IV; Perceptive Instruments, UK) attached to a fluorescence microscope (BX51, Olympus, Japan) and a Marlin F-046 CC camera. Images from 200 cells (100 from each replicate slide) were analyzed.

2.6. γ-H2AX/53BP1 FOCI METHOD

γ-H2AX represents a very sensitive marker of double strand DNA breaks. The complementary staining of the 53BP1 increases the method specificity, by co-visualization of two proteins involved in the same process [25].

The staining was done by an immunofluorescence protocol similar to one described at section 2.1. Instead of cytoskeleton staining, the antibodies used here were: primary antibodies mouse IgG anti-γH2AX (Millipore, Germany) and rabbit IgG anti-53BP1 (Abcam, UK) 1:800, with corresponding secondary Alexa Fluor 488 conjugated donkey anti-mouse IgG 1:200 and Rhodamine Red (Jackson Immunoresearch, USA) conjugated donkey anti-goat IgG 1:200.

For scoring, at least, 200 nuclei/sample were analyzed, counting for each of them the foci stained the both fluorophores being counted.

2.7. MORPHOLOGICAL APOPTOSIS DETERMINATION

Cells were detached with trypsin, centrifuged, stained with a solution of Acridine Orange (10 µg/mL) and Ethidium Homodimer (10 µg/mL) for 20 minutes and fixed in 1 % paraformaldehyde. The cells are visualized on a slide, using a fluorescence microscope (BX51, Olympus, Japan), and analyzed by their morphology and staining. Green cells with normal nuclei are scored as viable cells; nuclear condensation, or shrinking of the cells is a marker of apoptosis while swollen red cells are recorded as necrotic. At least 300 cells/slide were analyzed.

2.8. STATISTICAL ANALYSIS

The data is calculated as mean +/– SEM from a minimum of three experiments. Statistical significance is evaluated by Student t-test performed between irradiated and appropriate control samples and differentiated and appropriate undifferentiated cells. Statistical significance is considered at $p < 0.05$.

3. RESULTS

3.1. CONFIRMATION OF CELLULAR DIFFERENTIATION

Morphological observation indicates a progressive differentiation of cells during the incubation with RA-supplemented medium, revealed by progressive

formation and elongation of neurites, and decreased cellular proliferation (Fig. 1). Fluorescent staining of neuronal/non-neuronal markers sustains differentiation, by progressive expression of neuronal beta-III-tubulin protein, concomitant with loss of synthesis of the non-neuronal cytoskeleton component – actin.

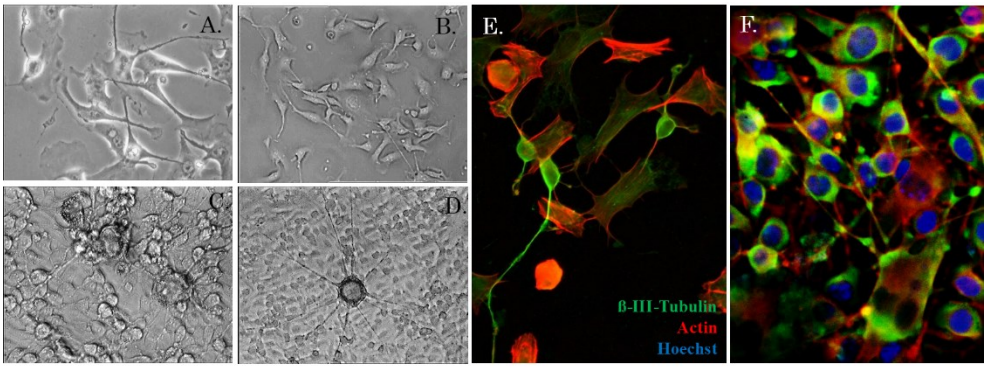

Fig. 1 – Cellular morphology and expression of differentiation marker: A, D – images of contrast phase microscopy of SH-SY5Y cultures (unstained); A, C – 200 × magnification. B, D – 100 × magnification; E, F – images obtained by fluorescence microscopy of SH-SY5Y cells stained with fluorescent markers for DNA (blue), actin filaments (red) and ß-III-tubulin (green). 400 × magnification; A, B, – cells in normal growth conditions at different magnifications; C, D, F – SH-SY5Y cells at 7 days of differentiation at different magnification; E – SH-SY5Y cells at 3 days of growth in differentiation medium.

3.2. COMET ASSAY

Comet assay represents a sensitive method for detection of genotoxic lesions, by single cell DNA electrophoresis, resulting in the migration of DNA fragments depending on their size proportional to the DNA fragmentation [24].

The method revealed higher DNA damage induction immediately following irradiation in differentiated cells, which show a tail intensity of 1.6 times higher as compared to undifferentiated cells. The DNA lesions are enhanced over time in the first period following irradiation, going to a tail intensity of 60 % for differentiated sample and 49 % in undifferentiated ones. This is a normal process involved in the first phases of repair mechanism. Later on the lesions tend to stagnate, showing that at the dose used (2.150 mJ) the cells were not able to repair the damage in none of the variants, at least for up to 3 hours post-exposure (Fig. 2). At later times post-exposure we have proved apoptosis induction, a process that involve DNA fragmentation interfering with comet assay so that we could not use the method at further times.

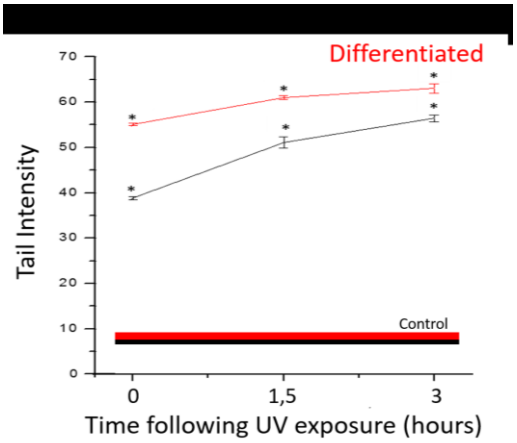

Fig. 2 – Comet assay analysis at progressive time immediately after exposure (0) to 3 hours following UV irradiation at 2.15 mJ/cm^2 (1 minute of exposure). Controls are marked as a line of mean +/– SEM Each point represents the mean of minimum 3 experiments +/– SEM; * $p < 0.05$ (student t-test).

3.3. γ-H2AX/53BP1

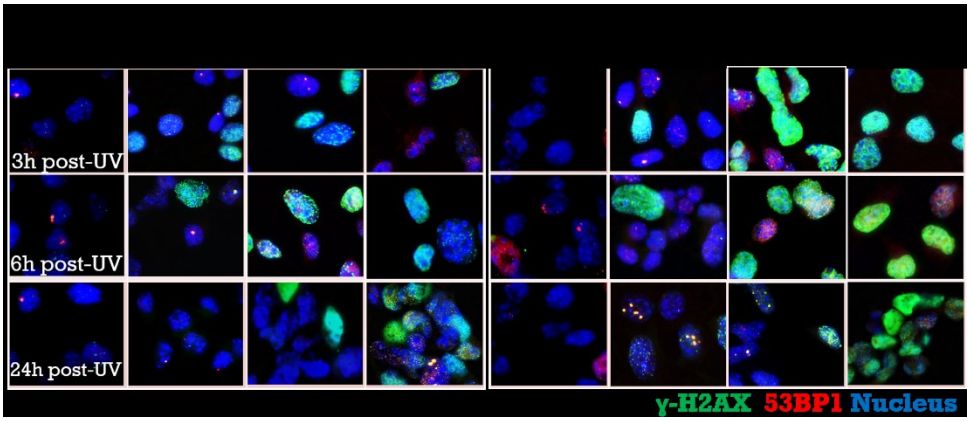

Fig. 3 – Representative images of γ-H2AX/53BP1 staining in SH-SY5Y cells. It is notable that at higher doses the cells become saturated with the stain, mainly in the differentiated form. Due to the very intense foci formation at doses of 1.075 and 2.150 mJ/cm^2, leading to inaccurate observation of individual foci, the scoring was only performed for the slides obtained at 0.358 mJ/cm^2.

γ-H2AX/53BP1 method shows the accumulation of proteins involved in DNA damage signaling and repair the lesions. The process involves a large DNA region in the surrounding of the lesion, being a very sensitive method. Following

repair, the γ-H2AX/53BP1 foci are cleaved, and the proteins return to their original form.

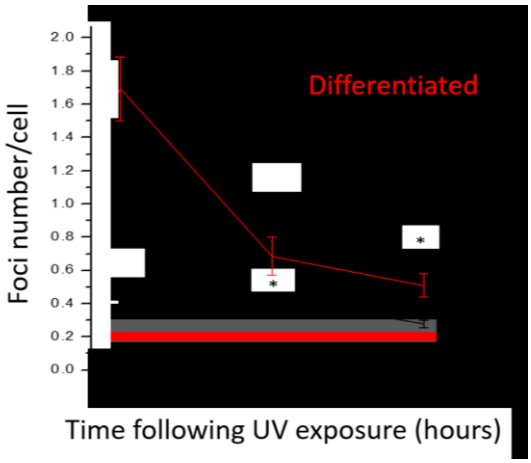

Fig. 4 – γ-H2AX/53BP1 foci measured at 3–24 hours following UV-irradiation at a dose of 0.358 mJ/cm^2 (10 seconds of exposure).
Controls are marked as a continuous line of their mean +/– SEM.
Each point represents mean of minimum 3 experiments +/– SEM; * $p < 0.05$ (student t-test).

We analyzed foci formation from 3 hours to 24 hours post-UV exposure, for a dose of 0.358 mJ/cm^2. At the higher doses as those used in the comet assay analysis presented above, the nuclei become saturated with the green staining that corresponds to γ-H2AX. The observation suggests a very high level of DSB DNA lesions, but an accurate scoring is impossible due to overlapping of individual foci. In Fig. 3 the representative images of γ-H2AX/53BP1 staining at progressive time and dose of UV-exposure, in SH-SY5Y cells, are shown.

Foci evolution showed a high increase at 3 hours post-irradiation for differentiated cells, from 0.19 foci/cells in control sample to 1.69 foci/cell in UV exposed, and a much lower response in the case of undifferentiated variant, were UV induces only 0.412 foci/cell starting with a similar control (Fig. 4). Even if the differentiated cells showed a response of 4.1 times higher than proliferative cells, in both cases, the cells repair the lesions. Still, in differentiated cells even at 24 hours post-irradiation, the residual level of γ-H2AX/53BP1 foci is statistically increased 2.6 fold as compared to the control cells showing in this case, an incomplete repair.

3.4. CELLULAR VIABILITY

Cellular viability was analyzed by MTS assay, at various time post UV-exposure: 3 hours, 6 hours, and 24 hours. At 3 hours post-irradiation cellular viability is not affected at the doses of 0.85 mJ/cm^2 or 1.70 mJ/cm^2 (Fig. 5).

At 6 hours post-irradiation, the cellular viability decreased at both doses in the case of differentiated cells to 88 % (at 0.85 mJ/cm^2) respectively 74 % (at 1.70 mJ/cm^2), and only at the higher dose in undifferentiated cells to 84 %. At 24 hours post-exposure, the cellular viability decreased more pronounced for both doses and cellular variants, the differentiated cells always showing a lower viability with only 35 % viability at 1.70 mJ/cm^2 compared with 60 % in the proliferative phenotype.

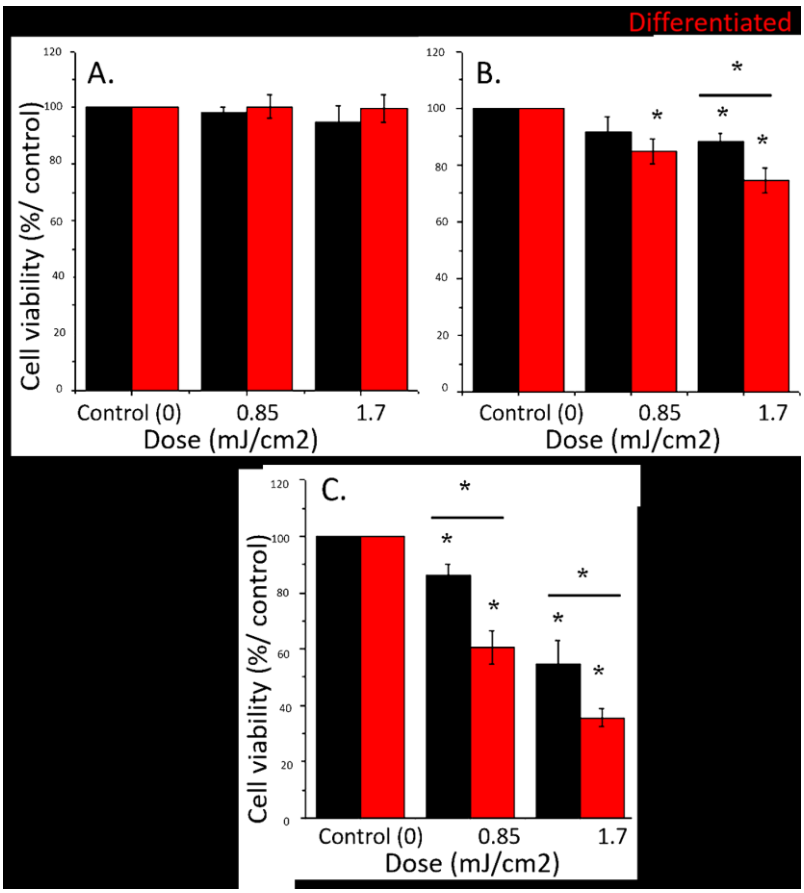

Fig. 5 – Cellular viability of SH-SY5Y cells at 3 hours (A.), 6 hours (B.) and 24 hours (C.) post-irradiation. Bars represent mean of minimum 3 experiments +/– SEM; * $p < 0.5$ (student t-test).

3.5. CASPASE 3/7 ACTIVATION

Caspase activation, a protein involved in apoptosis induction, was analyzed by measurement of caspase 3/7 level, at various time post UV-exposure: 3 hours, 6 hours, and 24 hours. At 3 hours post-irradiation we did not observe caspase

induction at the doses used of 0.850 mJ/cm^2 and 1.70 mJ/cm^2 (Fig. 6). At 6 hours post-irradiation, the caspase 3/7 activation is detected in differentiated cells at 1.70 mJ/cm^2 with a level of 1.45 times higher than control. At 24 hours, post-UV induction of caspase 3/7 is proved for both cell variants at 0.85 mJ/cm^2 and even more for 1.70 mJ/cm^2. Concerning the cell phenotypes, the differentiated variants showed an increased caspase 3/7 induction of 5.09 fold at 0.85 mJ/cm^2 and 7.44 fold at 1.70 mJ/cm^2 compared to undifferentiated cells, where the levels found were of 1.5 fold at 0.85 mJ/cm^2 and 5.71 fold at 1.70 mJ/cm^2.

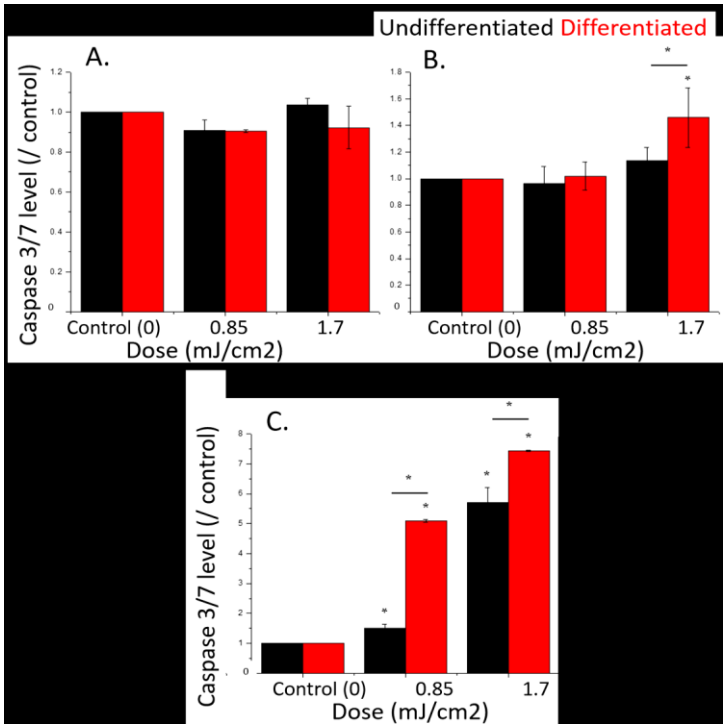

Fig. 6 – Caspase 3/7 activation in SH-SY5Y cells at 3 hours (A.), 6 and hours (B.) and 24 hours (C.) post-irradiation. Bars represent mean of minimum 3 experiments +/– SEM; * $p < 0.5$ (student t-test).

3.6. MORPHOLOGICAL APOPTOSIS

Morphological apoptosis measurements showed increased amount of apoptotic cells starting from 6 hours post-irradiation. In differentiated cells we found 10.33 % at 1.075 mJ/cm^2 and 16.16 % at 2.150 mJ/cm^2 compared with the control value of about 6 % apoptotic cells. The undifferentiated cells showed significant increase only for the higher dose of 2.15 mJ/cm^2 where 10 % of cells were apoptotic, compared to the control sample of 5 % apoptotic cells (Fig. 7). At 24 hours post-UV exposure, the apoptosis increased in both cell types at the

used doses, the differentiated cells showing apoptosis induction in up to 18 % of cells (at 2.150 mJ/cm^2).

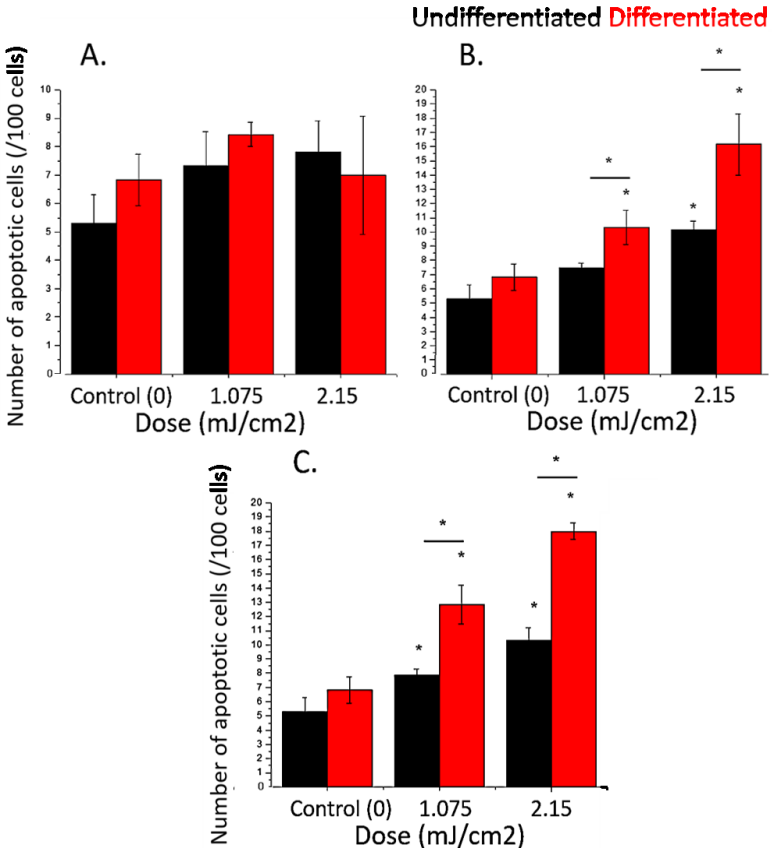

Fig. 7 – Morphological apoptosis of SH-SY5Y cells at 3 hours (A.), 6 and hours (B.) and 24 hours (C.) post-irradiation. Bars represent mean of minimum 3 experiments +/– SEM; * $p < 0.5$ (student t-test).

4. DISCUSSION

Overall, our study indicates a higher sensitivity to UV of differentiated cells compared to undifferentiated variants. Similar observations were revealed by studies on neuroblastoma [26, 27], neurons [9], adipocyte [28, 12]. On the other side, studies on cells of the immune system: T-lymphocytes [29] or myeloid leukemia cells [30] suggested a higher resistance of differentiated cells to genotoxic agents.

Prior UV exposure of neuronal cells, we changed the medium of all the cells to normal growth medium. This was done in order to prevent interference of soluble factors delivered by the cells in the medium composition with irradiation. In our case, serum and RA, the various medium components could lead to differences in UV absorbance or amount of reactive metabolites such as oxidative stress inductors. Analyzing DNA damages, immediately after UV exposure, we observed a slightly higher level of DNA lesions induced in RA differentiated neuronal cells compared to proliferative variant of the cell line. While at the higher doses of exposure used here, the DNA damages cannot be repaired, and the cells trigger apoptosis by caspase 3/7 activation, at lower dose of exposure, the DNA lesions are repaired over time.

Analysis of γ-H2AX/53BP1 foci shows increased damage in differentiated cells compared to undifferentiated at 3 hours post-exposure. The results are consistent with data from literature, that support a lower DNA repair capacity in neuronal differentiated cells [26, 27, 9]. A study performed on human neuroblastoma showed increased DNA damage induction by UV radiation together with lower repair capacity in differentiated cells [26]. Analysis of neuronal DNA repair also showed slower repair of pyrimidine-pyrimidone photoproducts and pyrimidine dimers in human neurons compared to precursor cells. In this case, the authors correlated this process with modulation of gene expression of several repair enzymes [9]. While immunofluorescent foci show pronounced differences between cellular variants compared to comet assay technique, we must keep in mind that in the 3 hours post-exposure the repair processes already started, which may indicate a faster repair in the proliferative cells. Also, γ-H2AX/53BP1 foci have a different kinetic than actual DNA lesion repair revealed by comet assay, the proteins being removed after the repair, by enzymatic activity, which may take various time intervals.

It is known that differentiated cells only express proteins required either in maintaining cellular homeostasis, or for their specific function, but they no longer replicate. The active genes are pruned to repair processes by transcription coupled repair that insure that the genetic information that is used, keep its integrity [31, 32]. While this mechanism only act during transcription, being useful for active genes, all the genetic material is normally subjected to other complex repair mechanisms [33]. The major repair pathways are NHEJ that is active through all the cell cycle [34] and HR that acts after replication, in G_2 phase of cell cycle [35]. Knowing that differentiated cells are blocked in the gap phase G_0, the HR pathways involved in DNA repair at check-point cannot be used. It appears that in differentiated cells the active genes are still repaired, even if the global DNA repair mechanisms are less activated [9]. This may be due to the fact that, given that the cells are terminally differentiated, their genetic material will not be further transcribed, and the chance that DNA lesions would induce mutations/ malignization is highly reduced.

At higher UV dose, DNA damages (2.15 mJ/cm^2) remain unrepaired, as shown by comet assay measurement and by visualization of the γ -H2AX/53BP1

slides, where a large part of the DNA was covered with the DSB-associated proteins, making the slides impossible to score.

Correlated with this, starting from 0.850 mJ/cm^2, we observed apoptosis induction by caspase 3/7 in differentiated cells, leading to loss of viability. Cellular death is dose and time dependent, significantly intensified in differentiated cells, where more cells are unable to repair their DNA lesions, for example at 24 hours post-exposure, caspase 3/7 levels are about 3.4 times higher in differentiated cells compared to undifferentiated cells at 0.850 mJ/cm^2. Other authors also recorded increased apoptosis in differentiated cells exposed to UV, compared to proliferative, working on keratinocytes, proving apoptosis induction by p53 activation [36], a protein involved in caspase pathway [37]. In that case, the increase in apoptosis induction was almost three times higher in differentiated cells as compared to undifferentiated variant [37].

5. CONCLUSIONS

In conclusion, our study proves that cellular differentiation increases UV sensitivity in SH-SY5Y dopaminergic neuronal model, impairing DNA repair and leading to apoptotic cellular death through caspase 3/7 activation.

Acknowledgments. We would like to thank Dr. Nicoleta Moisoi for providing the SH-SY5Y cell line used in the study. This study was supported by Romanian Ministry of Research National grants no. PN16420203, PN-II-ID-PCCE-2011-2-0027, PN-II-123/2012 and PN-II-98/2012. The funder had no involvement in the study design, collection, analysis and interpretation of data, writing the report and decision to submit the article for publication.

REFERENCES

1. M. Gentile, L Latonen, M Laiho, *Cell cycle arrest and apoptosis provoked by UV radiation-induced DNA damage are transcriptionally highly divergent responses*, Nucleic Acids Res. **31**(*16*), 4779-4790 (2003).
2. S.P. Jackson, J. Bartek, *The DNA-damage response in human biology and disease*, Nature **461**(*7267*), 1071-1078 (2009).
3. W.P. Ross, B. Kaina, *DNA damage-induced cell death: from specific DNA lesions to the DNA damage response and apoptosis*, Cancer Letters **332**(*2*), 237-248 (2013).
4. N.P. Restifo, M.E. Dudley, S.A. Rosenberg, *Adoptive immunotherapy for cancer: harnessing the T cell response*, Nature Reviews Immunology **12**, 269-281 (2012).
5. M. Paul, M.R. Goldsmith, J.R. Hunsley, F.C. Kafatos, *Specific protein synthesis in cellular differentiation. Production of eggshell protein by silkmoth follicular cells*, J. Cell Biol. **55**(*3*), 653-680 (1972).
6. M.H. Sherman, C.H. Bassing, M.A. Teitell, *Regulation of cell differentiation by the DNA damage response*, Trends in Cell Biology **21**(*5*), 312-319 (2011).
7. J.C. Lu, P.H. Lerou, G. Lahav, *Stem cells: balancing resistance and sensitivity to DNA damage*, Trends in Cell Biology **24**(*5*), 268-274 (2014).

8. M.V. Ferdousi, P. Rochereau, R. Chayot, B. Montagne, Z. Chaker, P. Flamant, S. Tajbakhsh, M. Ricchetti, *More efficient repair DNA double-strand breaks in skeletal muscle stem cells compared to their committed progeny*, Stem Cell Research **13**, 492-507 (2014).
9. T. Nouspikel, P.C. Hanawalt, *Terminally differentiated human neurons repair transcribed genes but display attenuated global DNA repair and modulation of repair gene expression*, Mol. Cell. Biol. **20**(*5*), 1562-1570 (2000).
10. P. Fortini, E. Dogliotti, *Mechanisms of dealing with DNA damage in terminally differentiated cells*, Mutat. Res. **685**(*1-2*), 38-44 (2010).
11. T. Nouspikel, *Some new answers to old questions*, Neuroscience **145**, 1213-1221 (2007).
12. C.A. Bill, M. Grochan, E.R. Meyn, V.A. Bohr, P.G. Tofilon, *Loss of intragenomic DNA repair heterogeneity with cellular differentiation*, J. Biol. Chem. **266**(*32*), 21821-21826 (1991).
13. S. Wingert, F.B. Thalheimer, N. Haetscher, M. Rehage, T. Schroeder, M.A. Rieger, *DNA-Damage response gene GADD45A induces differentiation in hematopoietic stem cells without inhibiting cell cycle or survival*, Stem Cells **34**(*3*), 699-710 (2016).
14. C.N. Weiss, I. Keisuke, *DNA Damage: A sensible mediator of the differentiation decision in hematopoietic stem cells and in leukemia*, Int. J. Mol Sci **16**, 6183-6201 (2015).
15. H.R. Xie, L.S. Hu, G.Y. Li, *SH-SY5Y human neuroblastoma cell line: in vitro cell model of dopaminergic neurons in Parkinson's disease*, Chin. Med. J. **123**(*8*), 1086-92 (2010).
16. J. Kovalevich, D. Langford, *Considerations for the use of SH-SY5Y neuroblastoma cells in neurobiology*, Methods Mol. Biol. **1078**, 9-21 (2013).
17. L. Agholme, T. Lindstrom, K. Kagedal, J. Marcusson, M. Hallbeck, *An in vitro model for neuroscience: differentiation of SH-SY5Y cells into cells with morphological and biochemical characteristics of mature neurons*, J. Alzheimer's Disease **20**(*4*), 1069-1082 (2010).
18. S. Dwane, E. Durack, P.A. Kiely, *Optimizing parameters for the differentiation of SH-SY5Y cells to study cell adhesion and cell migration*, BMC Research Notes **6**, 366 (2013).
19. J.I. Forster, S. Koglsberger, C. Trefois, O. Boyd, A.S. Baumuratov, L. Buck, R. Bailling, *Characterization of differentiated SH-SY5Y as neuronal screening model reveals increased oxidative vulnerability*, PMA Antony, J. Biomolecular Screening **21**(*5*), 496-509 (2016).
20. A.J. Morton, C. Hammond, W.T. Manson, G. Henderson, *Characterization of the L- and N-type calcium channels in differentiated SH-SY5Y neuroblastoma cells: calcium imaging and sigle channel recording*, Mol. Brain Res. **13**(*1-2*), 53-61 (1992).
21. K.P. Larrson, A.J. Hansen, S. Dissing, *The human SH-SY5Y neuroblastoma cell-line expresses a functional P2X7 purinoceptor that modulates voltage-dependent Ca^{2+} channel functions*, J. Neurochem. **83**(*2*), 285-298 (2002).
22. A.J. Roskamas, X. Cai, G.V. Ronnett, *Expression of neurons-specific beta-III-tubulin during olfactory neurogenesis in the embryonic and adult rat*, Neuroscience **83**(*1*), 191-200 (1998).
23. P. Stambolsky, Y. Taback, G. Fontemaggi, L. Weisz, R. Maor-Aloni, Z Sigfried, I. Kogran, M. Shay, E. Kalo, G. Blandino, I. Simon, M. Oren, V. Rotter, *Modulation of the vitamin D3 response by cancer-associated mutant p53*, Cancer Cell **17**(*3*), 273-85 (2010).
24. N.P. Singh, M.T. McCoy, R.R. Tice, E.L. Schneider, *A simple technique for quantitation of low levels of DNA damage in individual cells*, Exp. Cell Biol. **175**, 184-191 (1988).
25. M. Lassmann, H. Hanscheid, D. Gassen, J. Biko, V. Meinke, C. Reiners, H. Scherthan, *In vivo formation of gamma-H2AX and 53BP1 repair foci in blood cells after radioiodine therapy of differentiated thyroid cancer*, J. Nucl. Med. **51**(*8*), 1318-25 (2010).
26. M. James, J. Mansbridge, C. Kidson, *Ultraviolet radiation sensitivity of proliferating and differentiated human neuroblastoma cells*, Int. J. of Rad. Biol. and Relat. Stud. in Phys. Chem. and Med. **41**(*5*), 547-556 (1982).
27. M.F. Lavin, P. McCombie, C. Kidson, *DNA replication and post-replication repair in UV-sensitive mouse neuroblastoma cells*, Int. J. Radiat. Biol. Relat. Stud. Phys. Chem. Med. **30**(*1*), L31-40 (1976).
28. P.J. Tofilon, R.E. Meyn, *Influence of cellular differentiation on repair of ultraviolet-induced DNA damage in murine proadipocytes*, Radiat. Res. **116**(*2*), 217-27 (1988).

29. A. Cohen, C. Leung, *6-methylguanine-DNA methyltransferase activity and sensitivity to N-methyl-N'-nitro-nitrosoguanidine during human T-lymphocyte differentiation*, Carcinogenesis **7**(*11*), 1877-9 (1986).
30. T. Nakamaki, T. Ajiri, A. Sakashita, S. Tomoyasu, N. Tsuroka, *UV-induced DNA repair in leukemic cell differentiation*, J. Japan Haematol. Soc. **52**(*6*), 977-987 (1989).
31. T. Nouspikel, P.C. Hanawalt, *DNA repair in terminally differentiated cells*, DNA repair (Amst) **1**(*1*), 59-75 (2002).
32. N.J. Savery, *The molecular mechanism of transcription-coupled DNA repair*, Trends Microbiol **15**(*7*), 326-33 (2007).
33. M. Shrivastav, L.P. De Haro, J.A. Nickoloff, *Regulation of DNA double strand break repair pathway choice*, Cell Res. **18**, 134-147 (2008).
34. A.J. Davis, D.J. Chen, *DNA double strand break repair via non-homologus end-joining*, Transl Cancer Res. **2**(*3*), 130-143 (2013).
35. S.S. Foster, S. De, L.K. Johnson, J.H.J. Petrini, T.H. Stracker, *Cell cycle and DNA repair pathway-specific effects of apoptosis on tumor suppression*, PNAS **109**(*25*), 9953-9958 (2012).
36. V.A. Tron, M.J. Trotter, L. Tang, M. Krajewska, J.C. Reed, V.C. Ho, C. Li, *p53-regulated apoptosis is differentiation dependent in ultraviolet B-irradiated mouse keratinocytes*, Am. J. Pathol **153**(*2*), 579-585 (1998).
37. M. Schuler, D.R. Green, *Mechanisms of p53-dependent apoptosis*, Biochem. Soc. Transact. **29**(*6*), 684-688 (2001).